Extended abstract for Thermophysics Conference at AIAA Aviation 2019, June 17-21, 2019, Dallas, TX

Laser-Enhanced Arc-Jet Facility Wedge Tests: Avcoat Material Performance Under Convective and Radiative Heating Environments

Antonella I. Alunni*, Tahir Gökçen†, and Tane Boghozian‡
NASA Ames Research Center, Moffett Field, CA 94035

This paper presents the first set of experimental results from Laser Enhanced Arc-Jet Facility (LEAF-Lite) tests that were conducted shortly after the radiative LEAF-Lite system was added to the 60-MW Interaction Heating Facility at NASA Ames Research Center. Results were gathered to characterize the new radiative and combined heating capabilities as well as the convective heating resulting from the new IHF nozzle that was required for combined heating operations. Tests were ultimately conducted at several combinations of radiative and convective heating prompted by the need to understand the effect of combined heating on the Orion heatshield material prior to pursuing combined heating tests of the more complex block architecture.

I. Introduction

The Orion crew module will follow a Lunar-return trajectory during Exploration Missions 1 and 2 (EM-1 and EM-2). The large vehicle size and high reentry velocity will result in shock layer radiation emissions in vacuum ultraviolet (VUV) and infrared (IR). Preliminary studies for Orion have shown the radiative heating rate can be as high as the convective heating rate during peak heating, with VUV contributing up to half of the total amount of radiative heat flux [1]. Consequently, the program requires Laser Enhanced Arc-Jet Facility (LEAF-Lite) testing of thermal protection systems (TPS), including the Avcoat-tiled heatshield and 3DMAT compression pads, for the certification of flight readiness of EM-2, the first crewed Orion mission.

The LEAF-Lite system was recently added to the 60-MW Interaction Heating Facility (IHF) at NASA Ames Research Center (ARC). Immediately after LEAF-Lite was certified for operations with two 50-kW continuous wave (CW) IR lasers, test runs were conducted with water-cooled calibration plates, a tile plate coated with reaction-cured glass (RCG), and Avcoat plates to demonstrate feasibility of testing. The purpose of this paper is to further characterize the environments and TPS material response observed during the first LEAF-Lite test campaign.

II. Test Description

A. LEAF-Lite

Though radiative heating during the Orion flight is expected to cover a broad spectral range, the output wavelength of the LEAF-Lite lasers is 1070-nm. Each laser has a maximum power output of 50-kW and is a CW, Ytterbium +3 doped fiber laser that is stored outside of the IHF building [2]. The fiber lasers are directed into the building and inside the Optical Enclosure (OE), where the laser beams are collimated to produce a spatially-uniform, square irradiance pattern that is reflected out of the OE, through the beam path enclosure, and into the West side of the IHF through a test chamber window. The laser beams could operate one at a

* Aerospace Engineer, Entry Systems and Vehicle Development Branch (TSS), MS 234-1, Member AIAA
† Senior Research Scientist, AMA Inc., Aerothermodynamics Branch (TSA), MS 230-2, Associate Fellow AIAA
‡ Senior Research Scientist, AMA Inc., Thermal Protection Materials Branch (TSM), MS 223-1

time, or they could be incoherently combined to produce up to 400 W/cm^2 of radiative heating across a 15.24-cm x 15.24-cm (6-in x 6-in) target area.

Five radiative heating conditions, summarized in Table 1, were produced with LEAF-Lite during the IHF 335 test series, and cold-wall heat fluxes (CWHF) for each condition were measured with a water-cooled copper calibration plate instrumented with six Gardon gages, shown in Figure 1. The calibration plate was surface-coated with black paint (namely VHT SP102, $\varepsilon = 0.95$) to reduce undesired reflections and increase absorption. Mass flow of cold test gas (air) was required during all radiative heating runs to remove ablative products from the test plate surface (especially later in the case of the Avcoat plates) thereby avoiding blockage of the laser beam during tests. Ultimately, the calibration plate data revealed uniform heating distributions across the plate for each condition.

Table 1. Summary of CWHF measurements, facility parameters, and laser beam power for five radiative heating conditions.

Condition	CWHF Cal 1 (W/cm^2)	CWHF Cal 2 (W/cm^2)	CWHF Cal 3 (W/cm^2)	CWHF Cal 4 (W/cm^2)	CWHF Cal 5 (W/cm^2)	CWHF Cal 3 (W/cm^2)	CWHF Cal 6 (W/cm^2)	Main Air Flow (g/s)	Add Air Flow (g/s)	Argon Flow (g/s)	Total Power Output (kW)
R1	32	32	32	32	32	32	32	160	50	12	6.7
R2	83	83	83	83	83	83	83	160	50	12	17.7
R3	168	168	168	168	168	168	168	160	50	12	35.7
R4	340	340	340	340	340	340	340	160	50	12	72.5
R5	391	391	391	391	391	391	391	160	50	12	90.4

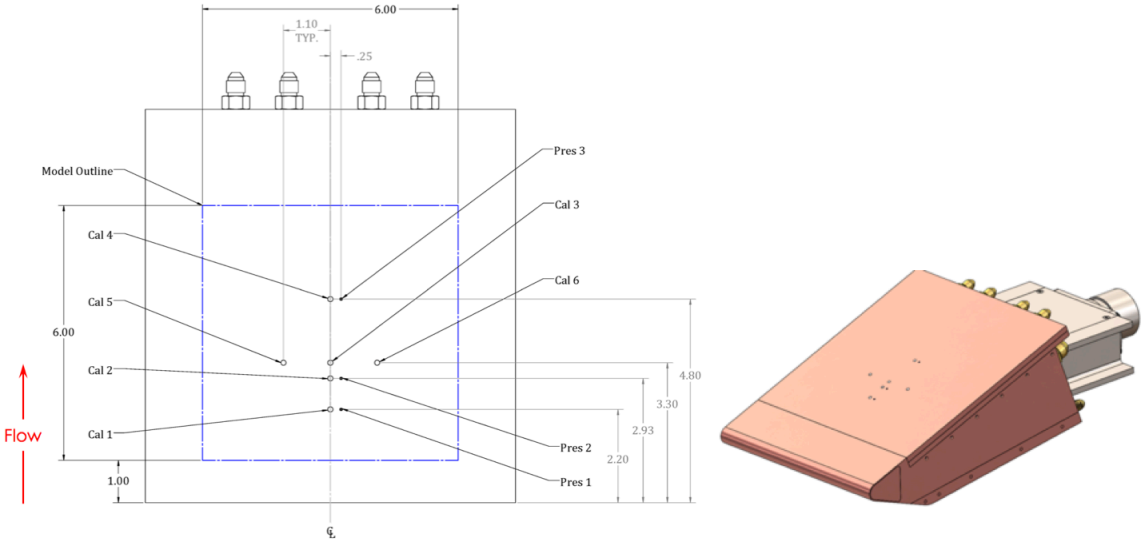

Figure 1. On left, water-cooled calibration plate drawing with dimensions in inches. Location of Gardon gages denoted by *Cal*, pressure transducers denoted by *Pres*, and laser beam target area outlined in blue. On right, assembly drawing of plate mounted onto a water-cooled wedge holder. Note that the radiative calibration plate was not instrumented with pressure sensors while the convective calibration plate did include pressure sensors.

B. Arc-Jet Facility

The IHF comprised a 60-MW segmented arc heater that included a new add-air plenum, which was introduced to shift add-air injection downstream of the last electrode and improve mixing at the nozzle inlet, and a new conical nozzle with 22.86-cm (9-inch) exit diameter and 6.033-cm (2.375-in) throat diameter [3]. This nozzle was introduced to maximize convective heating across the 15.24-cm x 15.24-cm LEAF-Lite target area.

During IHF 335 tests, the wedge models were tested at three convective heating conditions (summarized in Table 2). CWHF for each condition were measured with a water-cooled copper calibration plate, illustrated in Figure 1. The plate dedicated to calibrating convective heating was similar to the one used for radiative conditions except that the convective plate included three pressure transducers located near the centerline of the plate and the surface of the plate was uncoated. The convective calibration plate data exhibited decay in both heat flux and pressure along the wetted length, indicating test gas expansion over the plate.

Both radiative and convective calibration plates were installed into 20-degree, half-angle, water-cooled copper wedges, illustrated in Figure 1, that were mounted vertically with the plate facing West in the test chamber to enable LEAF-Lite testing.

Corresponding computational fluid dynamics (CFD) simulations were performed, and estimates of the centerline total enthalpy, shear, and hot-wall heat flux (HWHF) ranging from 2.54-cm from the leading edge of the calibration plate (which corresponds to the leading edge of the LEAF-Lite target or TPS test plate) to 15.24-cm downstream are summarized in Table 3. The nozzle upgrade to the IHF and corresponding CFD analyses of the arc-jet tests are discussed in further detail in a companion paper to be submitted to AIAA in June 2019 [4].

Table 2. Summary of CWHF, pressure measurements, and facility parameters for three convective heating conditions.

Condition	CWHF Cal 1 (W/cm^2)	CWHF Cal 2 (W/cm^2)	CWHF Cal 3 (W/cm^2)	CWHF Cal 4 (W/cm^2)	CWHF Cal 5 (W/cm^2)	CWHF Cal 3 (W/cm^2)	CWHF Cal 6 (W/cm^2)	P1 (kPa)	P2 (kPa)	P3 (kPa)	Arc Current (A)	Main Air Flow (g/s)	Add Air Flow (g/s)	Argon Flow (g/s)
C1	39	33	32	28	32	32	35	1.69	1.54	1.12	2036	80	50	14
C2	106	88	83	76	79	83	81	6.71	6.11	4.93	2831	381	55	32
C3	193	160	143	144	152	143	142	14.43	13.16	10.86	6017	740	50	53

Table 3. Summary of CFD estimates, centerline total enthalpy, and surface quantities along the test plate centerline.

Condition	CWHF Computed (W/cm^2)	HWHF Computed (W/cm^2)	P Computed (kPa)	Shear Computed (kPa)	Enthalpy Computed (MJ/kg)
C1	43 - 23	36 - 21	1.90 - 1.04	73 - 46	15.4
C2	117 - 61	94 - 55	7.7 - 4.1	163 - 106	18.9
C3	223 - 116	181 - 105	16.2 - 8.7	248 - 165	24.2

C. Combined Heating

After radiative and convective conditions were calibrated separately, a subset of radiative and convective conditions was combined to produce total heat fluxes with varying ratios of convective to radiative heating, as detailed in Table 4. These conditions, T1 through T3, were used exclusively for testing Avcoat. The combined heating runs adhered to the following sequence: the arc-jet operator tuned into the desired convective condition and activated the sting arm to swing into nozzle centerline, at which point the programmed lasers would automatically turn on.

Table 4. Summary of combined heating conditions, corresponding facility parameters, and laser beam power.

Condition	CWHF Cal 2, Convective (W/cm^2)	CWHF Cal 2, Radiative (W/cm^2)	P2 (kPa)	Arc Current (A)	Main Air Flow (g/s)	Add Air Flow (g/s)	Argon Flow (g/s)	Bulk (Sonic Flow) Enthalpy (MJ/kg)	Total Power Output (kW)
T1 (C2 + R2)	88	83	6.11	2831	381	55	32	15.9	17.7
T2 (C3 + R3)	160	168	13.16	6017	740	50	53	21.0	35.7
T3 (C3 + R4)	160	340	13.16	6017	740	50	53	21.0	72.5

D. Test Plates

The radiative and convective copper calibration plates granted limited coverage of the LEAF-Lite target area, so an LI-2200 tile coated with RCG and instrumented with 17 R-type, near-surface thermocouples (TCs), displayed in Figure 2, was tested to expand upon the characterization of the target area. The 15.24-cm x 15.24-cm plate was surrounded by carbon phenolic close-outs such that the plate area was in alignment with the LEAF-Lite target area. Due to failure of tile and RCG coating at relatively low heat fluxes, this plate was only tested at the lowest radiative and the lowest convective conditions.

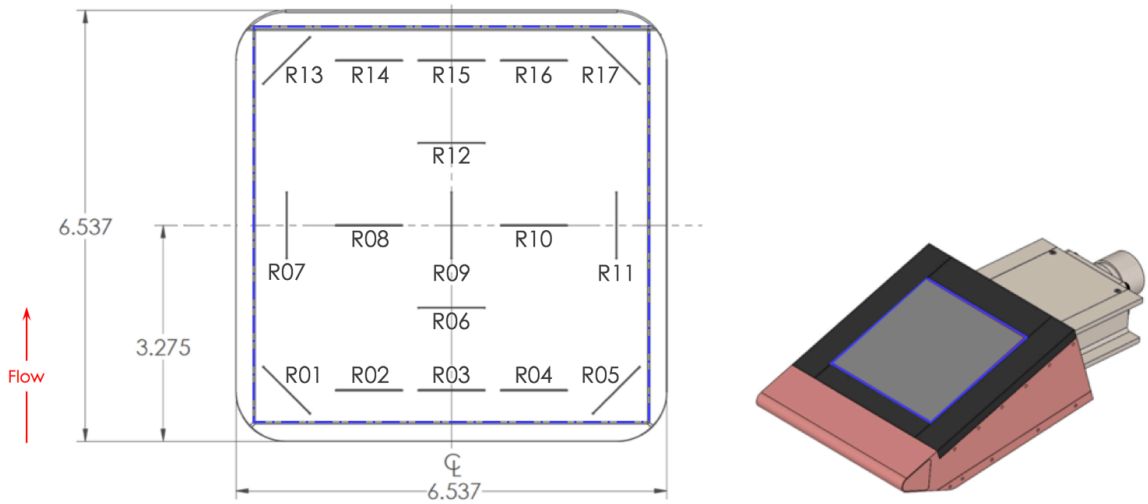

Figure 2. On left, RCG-coated tile plate drawing with dimensions in inches. Solid black lines illustrate land-length locations of R-type TCs, and laser beam target area is outlined in blue. On right, assembly drawing of tile plate mounted onto a water-cooled wedge holder.

The test campaign also included runs of Avcoat test plates, each instrumented with a single, 2.54-cm diameter thermocouple plug, including three R-type and 3 K-type in-depth TCs. Each plug was located 4.902-cm (1.930-in) from the leading edge of the test plate, which corresponds to the same location as Cal 2 on the water-cooled calibration plates, as noted in Figure 3. Like the RCG-coated tile plate, each Avcoat plate was surrounded with carbon phenolic close-outs, and the 15.24-cm x 15.24-cm surface area of Avcoat lined up with the LEAF-lite target area. Avcoat test plates were tested at the moderate radiative condition R3, the highest convective condition C3, and all combined heating conditions, T1 through T3.

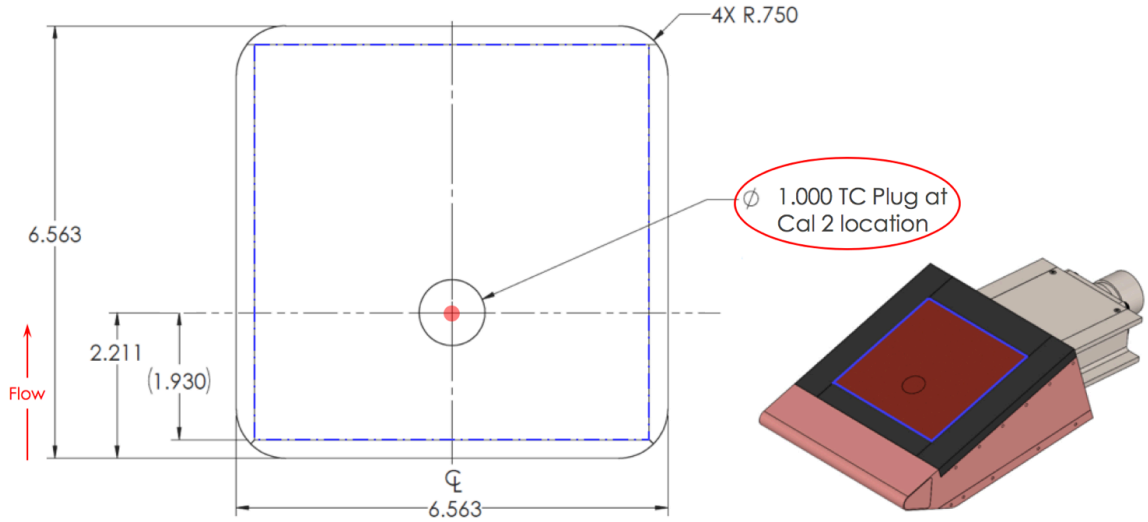

Figure 3. On left, Avcoat plate drawing with dimensions in inches, illustrating location of the in-depth TC plug. On right, assembly drawing of Avcoat plate mounted onto a water-cooled wedge holder.

III. Test Results

When the RCG-coated tile was run at convective condition C1, surface temperature gradients were observed along the wetted length of the test plate, as shown in Figure 4 and comparable to heat flux gradients observed during the convective calibration plate runs. Meanwhile, tile surface temperatures observed at condition R1, also displayed in Figure 4, were predominantly uniform across the test plate, similar to uniform heating observed during the radiative calibration plate run. Though note that TC temperatures were extraordinarily lower at one of the edges of the test plate, indicating that the beam path had drifted off-target (which was corrected after this run).

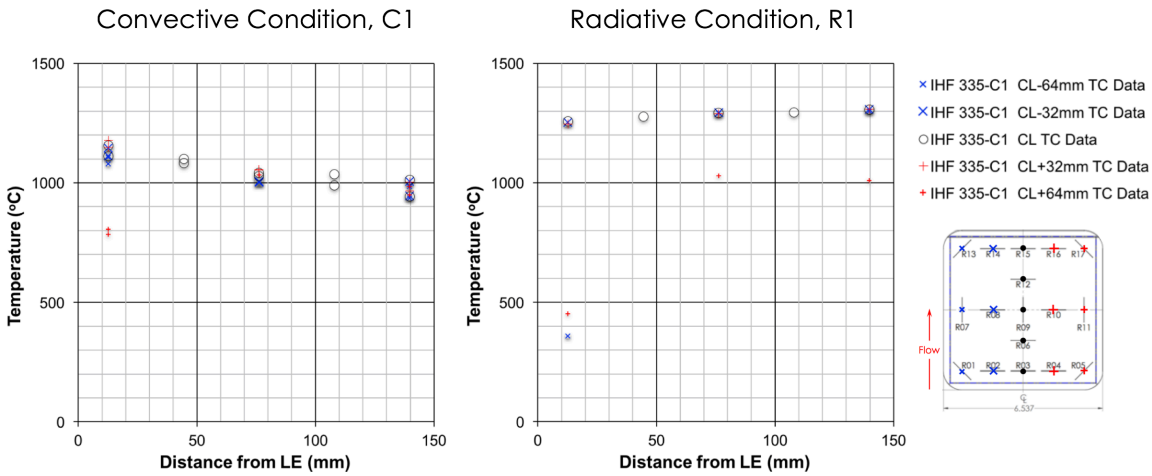

Figure 4. On left, surface temperatures measured during the low convective run using the RCG calibration plate, displaying streamwise decline in temperature across the test plate. On right, surface temperatures measured during the low radiative run using the RCG calibration plate, showing fairly uniform temperature distribution across most of the test plate.

At the end of IHF 335, Avcoat was evaluated at several different conditions. Avcoat test plates were run at convective condition C3, radiative condition R3, and combined heating condition T1 for 120 seconds at nominally 160 W/cm^2 CWHF to observe distinctions amongst the different modes of heating. Though note that all conditions differed in HWHF, where lowest HWHF was observed in in C1. Nonetheless, some distinguishing differences were observed from each post-test Avcoat surface, displayed in Figure 5.

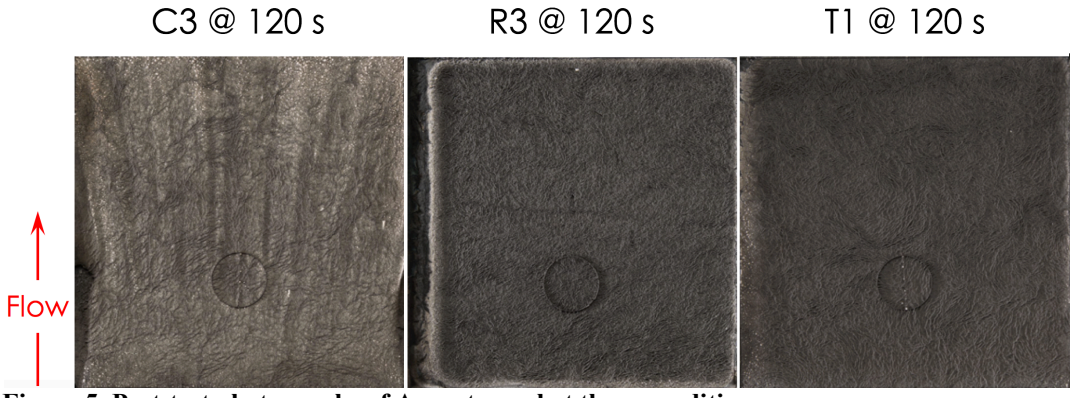

Figure 5. Post-test photographs of Avcoat panel at three conditions.

The convective heating Avcoat sample appeared the lightest in color because of the large amount of glass on the surface, which was only hot enough for glass melt to accumulate. Also, the convective heating Avcoat sample was abound with streamwise vortices, which are artifacts that are associated with shear arc-jet tests. Meanwhile, the radiative and combined heating samples had darker chars, which were sufficiently hot enough to vaporize the glass, and were free of typical shear test surface features.

Avcoat test plates run at combined heating conditions T2 and T3, shown in Figure 6, were exposed to twice the amount of convective heating as the T1 test plate. The higher convective heating contribution resulted in a higher degree of streamwise vortices observed at T2 and T3 compared to T1. Nevertheless, Avcoat tested at T2 and T3 contained no glass melt on the surface.

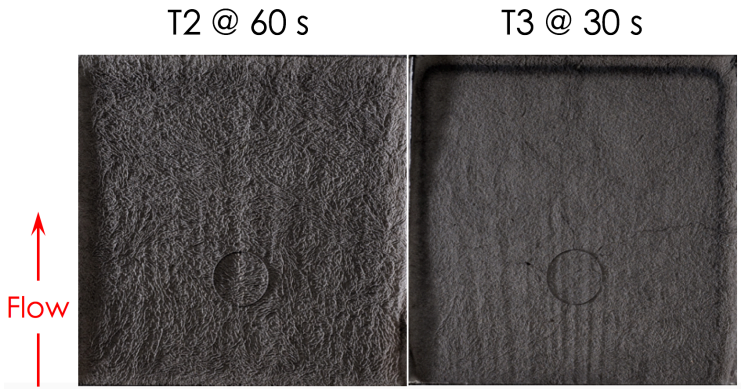

Figure 6. Post-test Avcoat surfaces resulting from runs at T2 and T3.

For samples tested at nominally 160 W/cm^2, the convective Avcoat test plate exhibited the highest amount of recession followed by the combined Avcoat test plate, as expected and shown in Figure 7. The radiative Avcoat plate had the lowest amount of recession, however, recession was not negligible. Since the IHF could not support runs with inert test gas, radiative testing in air inevitably resulted in oxidation and thus some amount of recession.

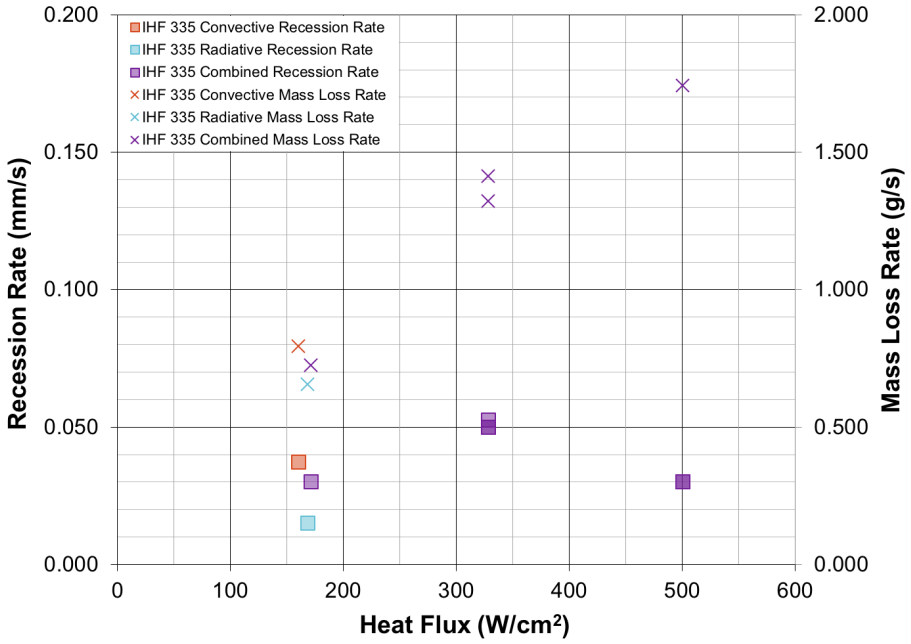

Figure 7. Variation of recession and mass loss rates with surface heat flux.

The mass loss rate of Avcoat rose with increasing CWHF, also demonstrated in Figure 7. However, the same positive trend was not observed with recession rate since the recession rate at the highest test condition, T3 (160 W/cm^2 convective with 340 W/cm^2 radiative) was equivalent to recession rate at the lowest combined condition, T1 (160 W/cm^2 convective with 160 W/cm^2 radiative). Char depths were measured for each sample, and the corresponding Avcoat charring rate results, displayed in Figure 8, varied positively with heat flux. The high mass loss rate at T3 was observed despite its low recession rate because the higher ratio of radiative to convective heating resulted in a higher quantity of in-depth heat absorption, as confirmed by the

higher charring rate. Further details on Avcoat thermal response, recession, mass loss, and char depth along with additional char assessments, including microstructural and elemental analyses, will be included in the full paper.

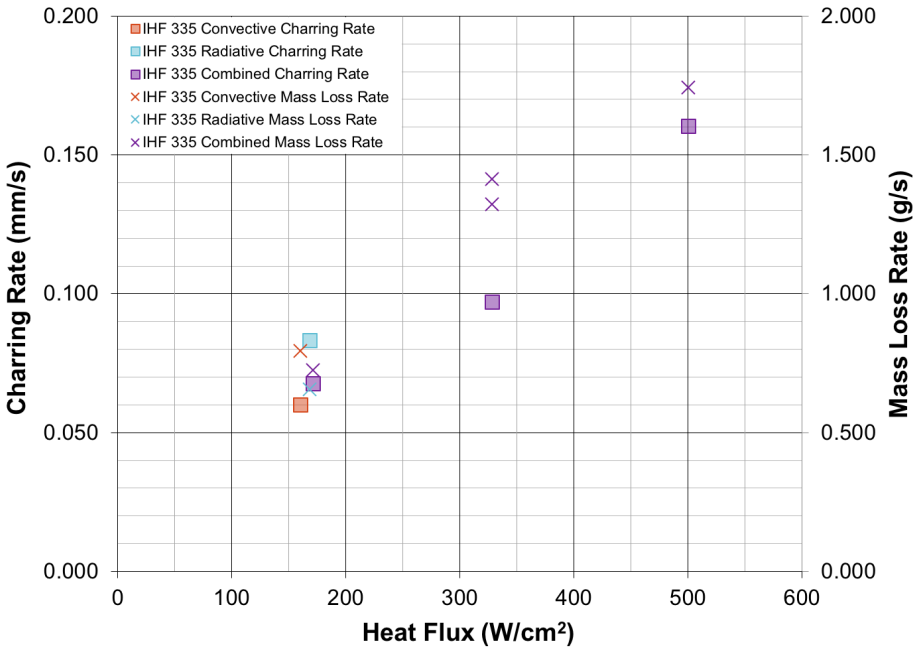

Figure 8. Charring rate and mass loss rate varying with heat flux for every Avcoat sample tested in IHF 335.

IV. Summary

The proposed paper describes Avcoat material performance results from the first LEAF-Lite wedge test campaign. LEAF-Lite and facility changes that allowed the IHF to accommodate this new capability are briefly described, and environments and RCG-coated tile and Avcoat runs performed in IHF 335 are discussed. Characterizations of Avcoat tested at purely radiative, purely convective, and varying quantities of combined heating were conducted to enable a practical understanding of TPS testing with LEAF-Lite. Furthermore, these assessments provide a baseline set of data and analysis for reference to inform future test campaigns ahead of the EM-2 TPS certification.

Acknowledgments

The authors gratefully acknowledge the support provided by the Orion TPS Insight and Oversight Project and NASA ARC Entry Systems and Technology Division through their NNA15BB15C to AMA Incorporated. The authors would also like to thank the LEAF-Lite Project and arc-jet test facility team at Ames and NASA-SCAP for their critical financial support of the arc jet operational capability at Ames.

References

[1] Bose, D., McCorkle, E., Thompson, C., Bogdanoff, D., Prabhu, D. K., Allen, G. A., and Grinstead, J., "Analysis and Model Validation of Shock Layer Radiation in Air," AIAA Paper 2008–1246, January 2008.

[2] Cushman, G., Alunni, A., Balboni, J., Zell, P., Hartman, J., and Empey, D., "The Laser Enhanced Arc-Jet Facility (LEAF-Lite): Simulating Convective and Radiative Heating with Arc-Jets and Multiple 50-kW CW Lasers," AIAA Paper 2018-3273, June 2018.

[3] Terrazas-Salinas, I., "Test Planning Guide for NASA Ames Research Center Arc Jet Complex and Range Complex," A029-9701-XM3 Rev. D, Thermophysics Facilities Branch, Space Technology Division, NASA Ames Research Center, January 2018.

[4] Gökçen, T., and Alunni, A., "CFD Simulations of the IHF Arc-Jet Flow: 9-Inch Nozzle, Flow Surveys, LEAF Wedge Calibration Data," Extended abstract submitted for Thermophysics Conference at AIAA Aviation 2019.